

THE GAUSSIAN BEAM METHOD FOR THE WIGNER EQUATION WITH DISCONTINUOUS POTENTIALS

DONGSHENG YIN^{*}, MIN TANG[†], AND SHI JIN[‡]

Abstract. For the Wigner equation with discontinuous potentials, a phase space Gaussian beam (PSGB) summation method is proposed in this paper. We first derive the equations satisfied by the parameters for PSGBs and establish the relations for parameters of the Gaussian beams between the physical space (GBs) and the phase space, which motivates an efficient initial data preparation thus a reduced computational cost than previous method in the literature. The method consists of three steps: 1) Decompose the initial value of the wave function into the sum of GBs and use the parameter relations to prepare the initial values of PSGBs; 2) Solve the evolution equations for each PSGB; 3) Sum all the PSGBs to construct the approximate solution of the Wigner equation. Additionally, in order to connect PSGBs at the discontinuous points of the potential, we provide interface conditions for a single phase space Gaussian beam. Numerical examples are given to verify the validity and accuracy of method.

Key words. Gaussian beam, Wigner equation, Discontinuous potential, Interface condition

AMS subject classifications. 65M75, 81Q20, 35Q41

1. Introduction. In this paper we present a phase space Gaussian beam method for solution of the Wigner equation. The Wigner equation describes quantum transport in semiconductor materials and can be derived from the density matrix formulation of quantum mechanics. It describes the time evolution of the Schrödinger equation using the Wigner Distribution Function [42]

There are two main reasons for using the Wigner formulation in applications. First, thanks to its form of a quantum Boltzmann equation, the Wigner equation can model the scattering phenomena. Second, inspired from classical kinetic models [10], the quantum-kinetic formulation makes it easier to construct boundary conditions at the device contacts.

The Wigner function is widely used in describing the properties of electronic devices such as the Resonant Tunneling Diode (RTD) and others [10]. The Wigner model is often employed to determine the current-voltage characteristic of these devices as well as their behavior away from equilibrium. Previous efforts in the simulations of Wigner equation can be put into two categories, one is deterministic, the other is the Monte Carlo method. The earliest numerical simulations in the mid-1980s were based on finite-difference schemes [10, 15, 33]. In 1990s, spectral collocation methods were developed as an efficient improvement for the discretization of the nonlocal operator $\mathcal{L}^\epsilon W^\epsilon$ [34]. In [35] an operator-splitting technique for the transport term $\mathbf{k} \cdot \nabla_{\mathbf{x}}$ and the pseudo-differential term were used to solve the Wigner equation. An analysis of the discrete-momentum Wigner model was performed in [5, 12]. A deterministic par-

^{*}Department of Mathematical Sciences, Tsinghua University, Beijing 100084, P.R. China(dyin@math.tsinghua.edu.cn). D. Yin was supported by NSFC grant No.10901091 and NSFC grant No.60873252.,

[†]Department of Mathematics and Institute of Nature Science, Shanghai Jiao Tong University, Shanghai 200240, P. R. China(tangmin@sjtu.edu.cn).,

[‡] Department of Mathematics, Institute of Nature Science, and Ministry of Education Key Laboratory in Scientific and Engineering Computing, Shanghai Jiao Tong University, Shanghai 200240, P. R. China, and Department of Mathematics, University of Wisconsin, Madison, WI 53706, USA(jin@math.wisc.edu), Shi jin was partially supported by NSF grant No. DMS- 1114546, and NSF RNMS grant No. 1107291. SJ was also supported by a Vilas Associate Award from University of Wisconsin-Madison.

title method for the Wigner equation was proposed and analyzed in [3]. The Monte Carlo method was studied from 2002 [27, 37], which allows the inclusion of more detailed scattering processes. For more recent results and advances about the Monte Carlo method, see [19, 28] and the review paper [38]. The Monte Carlo method has the potential to make multi-dimensional simulations feasible.

The Gaussian beam method (GB), which was first developed for the Schrödinger equation by Heller in 1970s [13], and independently developed by Popov for the linear wave equation [30], is an efficient approach that allows accurate computation of the amplitude near caustics. Similar to the classical ray tracing method, the Gaussian beam solution in physical space for the Schrödinger equation also has a WKB form. The center of the Gaussian beam follows the ray determined by a Hamiltonian system. The difference lies in that the Gaussian beam allows the phase function to be complex off its center, and the imaginary part of the phase function is positive, which makes the solution decay exponentially away from the center. The validity of the Gaussian beam method at caustics was analyzed by Ralston in [32]. Its uniform convergence was proved by Robert [36] recently.

The accuracy of the beam is determined by the truncation error of the Taylor expansion, and the approximate solution is given by a sum of all the beams. The accuracy of the Taylor expansion was studied by Motamed and Runborg in [26], and Tanushev in [41]. A Gaussian beam method was presented for the analysis of the energy of the high frequency solution to the mixed problem of the scalar wave equation in a convex domain by Akian, Alexandre, Bougacha in [1]. By computing Wigner measures based on the Gaussian beam formalism, they obtained more accurate asymptotic estimates for the limit of the energy of the waves than methods based on pseudo-differential calculus. Higher order Gaussian beam method that give better accuracy for the linear wave equations was developed and analyzed in [41]. Also for the Schrödinger equations, Yin and Zheng [43] constructed a high order Gaussian beam method and derived the interface conditions for the discontinuous potentials. Eulerian Gaussian beam methods were developed in [18, 20, 21]. See also a recent review on numerical solutions of semiclassical limit of high frequency waves [16]. Accuracy studies were carried out in [8, 23]. New initial data decomposition methods were developed in [2, 31, 39, 44].

In this paper, we propose a phase space Gaussian beam (PSGB) method for the Wigner equation. We first derive the equations satisfied by the parameters for PSGBs and establish the relations of parameters for Gaussian beams between physical space (GBs) and the phase space. This gives efficient initial data preparation which yields a computational cost lower than previous method in the literature [14]. The method consists of three steps: 1) Decompose the initial value of the wave function into the sum of GBs and use the parameter relations to get the initial values of PSGBs; 2) Solve the evolution equations for each PSGB; 3) Sum all the PSGBs to construct the approximate solution of the Wigner equation. Additionally, in order to connect PSGBs at the discontinuous points of the potential, we establish interface conditions for a single PSGB. Compared to the PSGB method for the one dimensional Liouville equations with quantum initial conditions in [14], our approach requires the number of PSGBs to be $O(\epsilon^{-\frac{n}{2}})$ instead of $O(\epsilon^{-n})$, thus significantly reduces the computational cost.

One may argue that the Wigner equation is defined in the phase space, thus an approximate method such as the PSGB method is much more expensive than a GB method for the original Schrödinger equation. This is true in the pure state case.

However, for mixed state, one needs to use the von Neumann equation, which doubles the dimension anyway, while the Wigner equation has the same dimension. This is another motivation for the PSGB other than those mentioned earlier.

The paper is organized as follows. In Sec. 2, we introduce the PSGB formulation for the Wigner equation and study the relations between GBs and PSGBs. In Sec. 3, we give the interface conditions at the discontinuous points of the potential. The strategies to implement the PSGBs summation are illustrated in Sec. 4. To demonstrate the accuracy and efficiency of our PSGB method, numerical examples of both one and two space dimensions are given in Sec. 5. Finally, we make some conclusive remarks in Sec. 6.

2. The Gaussian beam method for the Wigner equation.

2.1. The Wigner equation. The Wigner equation can be derived from the Schrödinger equation using the Wigner transform. Consider the following Schrödinger equation,

$$(2.1) \quad i\epsilon\psi_t^\epsilon(t, \mathbf{x}) = -\frac{1}{2}\epsilon^2\Delta\psi^\epsilon(t, \mathbf{x}) + V(\mathbf{x})\psi^\epsilon, \quad \mathbf{x} \in \mathbb{R}^d, t > 0,$$

$$(2.2) \quad \psi^\epsilon(0, \mathbf{x}) = \psi_0^\epsilon(\mathbf{x}) = A_0(\mathbf{x})e^{iS_0(\mathbf{x})/\epsilon},$$

where \mathbf{x} is the position, t is the time, $\psi(\mathbf{x}, t)$ is the complex-valued wave function, $V(\mathbf{x})$ is the potential and ϵ is the rescaled Plank constant.

The Wigner transform of ψ^ϵ is

$$(2.3) \quad W^\epsilon(t, \mathbf{x}, \mathbf{k}) = \frac{1}{(2\pi)^n} \int_{\mathbb{R}^n} e^{i\mathbf{k}\cdot\mathbf{y}} \psi^\epsilon(t, \mathbf{x} - \frac{1}{2}\epsilon\mathbf{y}) \overline{\psi^\epsilon(t, \mathbf{x} + \frac{1}{2}\epsilon\mathbf{y})} d\mathbf{y},$$

where $\bar{\psi}$ denotes the complex conjugate of ψ . Then the corresponding evolution equation for the Wigner distribution function $W^\epsilon(t, \mathbf{x}, \mathbf{k})$ is,

$$(2.4) \quad \partial_t W^\epsilon(t, \mathbf{x}, \mathbf{k}) + \mathbf{k} \cdot \nabla_{\mathbf{x}} W^\epsilon(t, \mathbf{x}, \mathbf{k}) + \mathcal{L}^\epsilon W^\epsilon(t, \mathbf{x}, \mathbf{k}) = 0,$$

where the operator \mathcal{L}^ϵ is defined by

$$(2.5) \quad \mathcal{L}^\epsilon W^\epsilon(t, \mathbf{x}, \mathbf{k}) = -\frac{i}{(2\pi)^n} \int_{\mathbb{R}^n} W^\epsilon(t, \mathbf{x}, \mathbf{p}) \left(\int_{\mathbb{R}^n} e^{i(\mathbf{k}-\mathbf{p})\cdot\mathbf{y}} \frac{1}{\epsilon} (V(\mathbf{x} + \frac{\epsilon}{2}\mathbf{y}) - V(\mathbf{x} - \frac{\epsilon}{2}\mathbf{y})) d\mathbf{y} \right) d\mathbf{p},$$

which is local in \mathbf{x}, t and nonlocal in \mathbf{k} . The initial data corresponding to (2.2) is $W^\epsilon(0, \mathbf{x}, \mathbf{k}) = W_0^\epsilon(\mathbf{x}, \mathbf{k})$, which is not necessary to be specified for this paper.

The above two formulations (2.1) and (2.3) give the evolution in the physical space and phase space respectively. In fact one can recover the physical observables from both the wave function ψ^ϵ and the Winger function W^ϵ , namely,

$$(2.6) \quad \text{position density } \rho^\epsilon = |\psi^\epsilon|^2 = \int_{\mathbb{R}^n} W^\epsilon(t, \mathbf{x}, \mathbf{k}) d\mathbf{k},$$

$$(2.7) \quad \text{density flux } J^\epsilon = \frac{\epsilon}{2i} (\psi^\epsilon \nabla \bar{\psi}^\epsilon - \bar{\psi}^\epsilon \nabla \psi^\epsilon) = \int_{\mathbb{R}^n} \mathbf{k} W^\epsilon(t, \mathbf{x}, \mathbf{k}) d\mathbf{k},$$

$$(2.8) \quad \text{kinetic energy } E^\epsilon = \frac{\epsilon^2}{2} |\nabla \psi^\epsilon|^2 = \int_{\mathbb{R}^n} |\mathbf{k}|^2 W^\epsilon(t, \mathbf{x}, \mathbf{k}) d\mathbf{k}.$$

When $V(\mathbf{x})$ is smooth enough and $\epsilon \rightarrow 0$, the Wigner equation converges to the Liouville equation [11, 22]

$$(2.9) \quad \partial_t W(t, \mathbf{x}, \mathbf{k}) + \mathbf{k} \cdot \nabla_{\mathbf{x}} W(t, \mathbf{x}, \mathbf{k}) - \nabla_{\mathbf{x}} V(\mathbf{x}) \cdot \nabla_{\mathbf{k}} W(t, \mathbf{x}, \mathbf{k}) = 0.$$

Moreover, if the initial data in the physical space have the WKB form (2.2), as $\epsilon \rightarrow 0$, the corresponding initial condition for the Liouville equation is

$$W(0, \mathbf{x}, \mathbf{k}) = |A_0(\mathbf{x})|^2 \delta(\mathbf{k} - \nabla S_0(\mathbf{x})).$$

2.2. The Gaussian beam method for the Schrödinger equation. Similar to the WKB method, the Gaussian beam solution is given in the form

$$(2.10) \quad \phi^\epsilon(t, \mathbf{x}, \mathbf{y}_0) = A(t, \mathbf{y}) e^{iT(t, \mathbf{x}, \mathbf{y})/\epsilon},$$

where the variable $\mathbf{y} = \mathbf{y}(t, \mathbf{y}_0)$ is the center of the beam, to be determined below, and the phase $T(t, \mathbf{x}, \mathbf{y})$ is given by

$$T(t, \mathbf{x}, \mathbf{y}) = S(t, \mathbf{y}) + \mathbf{p}(t, \mathbf{y}) \cdot (\mathbf{x} - \mathbf{y}) + \frac{1}{2}(\mathbf{x} - \mathbf{y})^T M(t, \mathbf{y})(\mathbf{x} - \mathbf{y}).$$

This is reminiscent of the Taylor expansion of the phase S around the point \mathbf{y} , upon identifying $\mathbf{p} = \nabla S \in \mathbb{R}^d$, $M = \nabla^2 S$, the *Hessian matrix*. The idea is to allow the phase T to be complex-valued, and keep the imaginary part of $M \in \mathbb{C}^{n \times n}$ positive definite so that (2.10) indeed has a Gaussian profile.

Plugging the ansatz (2.10) into the Schrödinger equation (2.1), and ignoring the higher-order terms in both ϵ and $\mathbf{x} - \mathbf{y}$, one obtains the following system of ODEs:

$$(2.11) \quad \frac{d\mathbf{y}}{dt} = \mathbf{p},$$

$$(2.12) \quad \frac{d\mathbf{p}}{dt} = -\nabla_{\mathbf{y}} V,$$

$$(2.13) \quad \frac{dS}{dt} = \frac{1}{2}|\mathbf{p}|^2 - V,$$

$$(2.14) \quad \frac{dM}{dt} = -M^2 - \nabla_{\mathbf{y}}^2 V,$$

$$(2.15) \quad \frac{dA}{dt} = \frac{1}{2}(\text{Tr}(M))A,$$

where \mathbf{p}, V, M, S and A are functions of $(t, \mathbf{y}(t, \mathbf{y}_0))$. Equations (2.11)-(2.12) are the classical Hamiltonian system defining the ray-tracing algorithms. Equations (2.11)-(2.15) define the Lagrangian formulation of the Gaussian beams.

In practical computation, the Gaussian beam summation method for the Schrödinger equation can be implemented in three steps:

1. Decompose the initial data into summation of Gaussian beams

$$\psi^\epsilon(0, \mathbf{x}) = \sum_{j=1}^N \phi_j^\epsilon(0, \mathbf{x});$$

2. Solve the evolution equations of the parameters (as in (2.11)-(2.15)) for each Gaussian beam, to find the evolution of each Gaussian beam;
3. Sum up these Gaussian beams to construct an approximation of the wave function ψ^ϵ .

2.3. The Lagrangian method in the phase space. In this section, we will construct the phase space Gaussian beam (PSGB) for the Wigner equation and derive its evolution equation. The basic idea of a Gaussian beam method is to locally approximate the potential of the Schrödinger equation by a quadratic form, and then find out the corresponding evolution dynamics of Gaussian beams. The similar idea can be extended to the Wigner equation. Let the density distribution function have the following PSGB form

$$(2.16) \quad W(t, \mathbf{x}, \mathbf{k}) = U(t, \mathbf{q}, \mathbf{p}) \exp\left(-\frac{1}{\epsilon} T(t, \mathbf{x}, \mathbf{k}, \mathbf{q}, \mathbf{p})\right), \quad \mathbf{x}, \mathbf{k} \in \mathbb{R}^n, \quad n = 1, 2, 3,$$

where T is defined as

$$(2.17) \quad T = \begin{bmatrix} \mathbf{x} - \mathbf{q}(t) \\ \mathbf{k} - \mathbf{p}(t) \end{bmatrix}^T \begin{bmatrix} N_{11}(t) & N_{12}(t) \\ N_{21}(t) & N_{22}(t) \end{bmatrix} \begin{bmatrix} \mathbf{x} - \mathbf{q}(t) \\ \mathbf{k} - \mathbf{p}(t) \end{bmatrix}, \quad N_{ij}(t) \in \mathbb{R}^{n \times n}, \quad i, j = 1, 2.$$

When the potential is a quadratic function of \mathbf{x} , i.e. $V(\mathbf{x}) = \mathbf{x}^T B \mathbf{x} + \mathbf{b} \cdot \mathbf{x} + c$, $\mathbf{x} \in \mathbb{R}^n$, the Wigner equation coincides with the classical Liouville equation. Therefore, if we approximate the potential $V(\mathbf{x})$ near \mathbf{q} by

$$V(\mathbf{x}) \approx V(\mathbf{q}) + \nabla_{\mathbf{x}} V(\mathbf{q}) \cdot (\mathbf{x} - \mathbf{q}) + \frac{1}{2} (\mathbf{x} - \mathbf{q})^T \nabla_{\mathbf{x}}^2 V(\mathbf{q}) (\mathbf{x} - \mathbf{q}),$$

in the neighborhood of (\mathbf{q}, \mathbf{p}) , the original Winger equation (2.3) reduces to the Liouville equation

$$(2.18) \quad \frac{\partial W}{\partial t} + \mathbf{k} \cdot \nabla_{\mathbf{x}} W - (\nabla_{\mathbf{x}} V(\mathbf{q}) + \nabla_{\mathbf{x}}^2 V(\mathbf{q}) (\mathbf{x} - \mathbf{q})) \cdot \nabla_{\mathbf{k}} W = 0.$$

We now try to find the evolution dynamics of PSGB (2.16) determined by (2.18). Define

$$\mathbf{y} = \begin{bmatrix} \mathbf{x} \\ \mathbf{k} \end{bmatrix}, \quad \boldsymbol{\xi} = \begin{bmatrix} \mathbf{k} \\ -(\nabla_{\mathbf{x}} V(\mathbf{q}) + \nabla_{\mathbf{x}}^2 V(\mathbf{q}) (\mathbf{x} - \mathbf{q})) \end{bmatrix}, \quad \mathbf{z} = \begin{bmatrix} \mathbf{q} \\ \mathbf{p} \end{bmatrix},$$

rewrite (2.18) as

$$(2.19) \quad \frac{\partial W}{\partial t} + \boldsymbol{\xi} \cdot \nabla_{\mathbf{y}} W = 0.$$

Note that \mathbf{z} depends on t . Inserting the PSGB form (2.16) into (2.18), and collecting the first two orders with respect to ϵ , one obtains

$$(2.20) \quad O\left(\frac{1}{\epsilon}\right) : \frac{\partial T}{\partial t} + \nabla_{\mathbf{z}} T \cdot \frac{\partial \mathbf{z}}{\partial t} + \boldsymbol{\xi} \cdot \nabla_{\mathbf{y}} T = 0,$$

$$(2.21) \quad O(1) : \frac{\partial U}{\partial t} + \nabla_{\mathbf{z}} U \cdot \frac{\partial \mathbf{z}}{\partial t} = 0.$$

Taking the first and second derivatives with respect to \mathbf{y} in (2.20) gives

$$(2.22) \quad \frac{\partial(\nabla_{\mathbf{y}} T)}{\partial t} + (\nabla_{\mathbf{y}} \mathbf{z} T)^T \frac{\partial \mathbf{z}}{\partial t} + (\nabla_{\mathbf{y}} \boldsymbol{\xi})^T \nabla_{\mathbf{y}} T + (\nabla_{\mathbf{y}}^2 T)^T \boldsymbol{\xi} = 0,$$

$$(2.23) \quad \frac{\partial(\nabla_{\mathbf{y}}^2 T)}{\partial t} + (\nabla_{\mathbf{y}} \mathbf{y} \mathbf{z} T)^T \frac{\partial \mathbf{z}}{\partial t} + (\nabla_{\mathbf{y}} \boldsymbol{\xi})^T \nabla_{\mathbf{y}}^2 T + (\nabla_{\mathbf{y}}^2 T)^T \nabla_{\mathbf{y}} \boldsymbol{\xi} + \nabla_{\mathbf{y}}^3 T = 0.$$

Let $\mathbf{y} = \mathbf{z}$ and noting (2.17), one has

$$\nabla_{\mathbf{y}} T|_{\mathbf{y}=\mathbf{z}} = 0, \quad \nabla_{\mathbf{y}\mathbf{z}} T|_{\mathbf{y}=\mathbf{z}} = -2N, \quad \nabla_{\mathbf{y}}^2 T|_{\mathbf{y}=\mathbf{z}} = 2N,$$

with

$$N = \begin{bmatrix} N_{11}(t) & N_{12}(t) \\ N_{21}(t) & N_{22}(t) \end{bmatrix},$$

so that (2.22) becomes

$$N \left(\frac{\partial \mathbf{z}}{\partial t} - \boldsymbol{\xi} \right) |_{\mathbf{y}=\mathbf{z}} = 0.$$

If N is nonsingular, then

$$(2.24) \quad \frac{\partial \mathbf{z}}{\partial t} = \boldsymbol{\xi} |_{\mathbf{y}=\mathbf{z}} = \begin{bmatrix} \mathbf{p} \\ -\nabla_{\mathbf{q}} V(\mathbf{q}) \end{bmatrix}.$$

Similarly when $\mathbf{y} = \mathbf{z}$, (2.23) becomes

$$(2.25) \quad \frac{\partial N}{\partial t} + \frac{\partial \mathbf{z}}{\partial t} \cdot \nabla_{\mathbf{z}} N + (\nabla_{\mathbf{y}} \boldsymbol{\xi})^T N + N^T \nabla_{\mathbf{y}} \boldsymbol{\xi} = 0.$$

Combining (2.21), (2.24) and (2.25), we obtain the ODE system describing the evolution of the parameters of the PSGB:

$$(2.26) \quad \frac{dN}{dt} = -[(\nabla_{\mathbf{y}} \boldsymbol{\xi})^T N + N^T \nabla_{\mathbf{y}} \boldsymbol{\xi}],$$

$$(2.27) \quad \frac{dU}{dt} = 0,$$

$$(2.28) \quad \frac{d\mathbf{q}}{dt} = \mathbf{p},$$

$$(2.29) \quad \frac{d\mathbf{p}}{dt} = -\nabla_{\mathbf{q}} V(\mathbf{q}).$$

To preserve the Gaussian profile, the matrix $N(t)$ must be positive definite. The equation (2.26) is the Lyapunov equation. Dieci and Eirola proved the following proposition in [9].

PROPOSITION 2.1. *The solution of the following Lyapunov equation*

$$(2.30) \quad \dot{X}(t) = C(t)X^T(t) + X(t)C^T(t) + D(t),$$

$$(2.31) \quad X(0) = X_0, \quad X_0 \text{ is symmetric,}$$

exists and is symmetric for all $t > 0$. Furthermore, if $X(s)$ or $D(s)$ is positive definite for some $s \geq 0$, then $X(t)$ is positive definite for all $t \geq s$.

Thus, if the initial data $N(0)$ is symmetric and positive definite, then $N(t)$ remains so for all $t > 0$, which implies that the Gaussian profile will be preserved for all $t > 0$.

2.4. Relations between the GBs and PSGBs. The ODE system (2.26)-(2.28) was derived in [14], but only the cases with smooth potentials were considered. Additionally, the computational cost of the initial data preparation in [14] is very expensive. In this section, we illustrate a new way of initial data preparation, which can significantly improve the efficiency.

Before going to the details of our initial data decomposition, we review the procedure used [14]. Firstly, the Monte Carlo method was employed to decompose the initial data into Gaussian wave packages in the physical space, namely,

$$\psi(x, 0) \approx \sum_{j=1}^N A_j \exp \left[-a_j(x - x_j)^2 + \frac{i}{\epsilon} k_j(x - x_j) \right].$$

Apply the Wigner transform on this approximation, which is further decomposed into Gaussian beams in the phase space via the Monte-Carlo method,

$$W^\epsilon(t, x, k) \approx \sum_{n=1}^M A_n \exp \left\{ -[a_n(x - x_n)^2 + 2b_n(x - x_n)(k - k_n) + c_n(k - k_n)^2] \right\}.$$

Finally, the ODEs (2.26)-(2.29) were solved for each beam. A large number of beams is required to approximate the initial data, and $O(1/\epsilon)$ beams are needed to approximate the Wigner function.

We will use the relation between the GB and PSGB to get a more efficient decomposition of the initial data.

Take the WKB initial data (2.2). According to [41], one can approximate the initial data by the sum of a series of GBs

$$\mathfrak{W}(\mathfrak{Q}, \mathbf{x}) = A(\mathbf{x}) e^{iS(\mathbf{x})/\epsilon} \approx \sum_{j=1}^N A_j \exp \left[\frac{i}{\epsilon} \left(S_j + \mathbf{p}_j \cdot (\mathbf{x} - \mathbf{q}_j) + \frac{1}{2} (\mathbf{x} - \mathbf{q}_j)^T M (\mathbf{x} - \mathbf{q}_j) \right) \right].$$

We now take the Wigner transform on the right side of (2.32). Introduce the general Wigner transform:

$$(2.33) \quad \mathfrak{W}[\psi_1, \psi_2] = \frac{1}{(2\pi)^n} \int_{\mathbb{R}^n} e^{i\mathbf{k} \cdot \tilde{\mathbf{x}}} \psi_1 \left(\mathbf{x} - \frac{\epsilon}{2} \tilde{\mathbf{x}} \right) \overline{\psi_2 \left(\mathbf{x} + \frac{\epsilon}{2} \tilde{\mathbf{x}} \right)} d\tilde{\mathbf{x}},$$

which is a bilinear operator of ψ_1 and ψ_2 .

First of all, we consider the Wigner transform of one single GB. The Wigner transform for the GBs of the form

$$\phi(t, \mathbf{x}) = A_0(\mathbf{q}) \exp \left[\frac{i}{\epsilon} \left(S(\mathbf{q}) + \mathbf{p} \cdot (\mathbf{x} - \mathbf{q}) + \frac{1}{2} (\mathbf{x} - \mathbf{q})^T M (\mathbf{x} - \mathbf{q}) \right) \right]$$

is

$$(2.34) \quad \begin{aligned} W^\epsilon(t, \mathbf{x}, \mathbf{k}) &= \frac{1}{(2\pi)^n} \int_{\mathbb{R}^n} e^{i\mathbf{k} \cdot \tilde{\mathbf{x}}} \phi \left(t, \mathbf{x} - \frac{\epsilon}{2} \tilde{\mathbf{x}} \right) \overline{\phi \left(t, \mathbf{x} + \frac{\epsilon}{2} \tilde{\mathbf{x}} \right)} d\tilde{\mathbf{x}} \\ &= \frac{1}{(2\pi)^n} \int_{\mathbb{R}^n} e^{i\mathbf{k} \cdot \tilde{\mathbf{x}}} |A_0|^2 e^{i[-\mathbf{p} - L(\mathbf{x} - \mathbf{q}) \cdot \tilde{\mathbf{x}} - \frac{\epsilon}{4} \tilde{\mathbf{x}}^T K \tilde{\mathbf{x}} - \frac{1}{\epsilon} (\mathbf{x} - \mathbf{q})^T K (\mathbf{x} - \mathbf{q})]} d\tilde{\mathbf{x}} \\ &= \frac{|A_0|^2}{(\pi\epsilon)^{n/2} |K|^{\frac{1}{2}}} \exp \left[-\frac{1}{\epsilon} (\mathbf{y} - \mathbf{z})^T \tilde{M} (\mathbf{y} - \mathbf{z}) \right] \end{aligned}$$

with $L = \text{Re}(M)$, $K = \text{Im}(M)$, $|K| = \det K$ and

$$\tilde{M} = \begin{bmatrix} K + L^T K^{-1} L & -L^T K^{-1} \\ -K^{-1} L & K^{-1} \end{bmatrix}.$$

From (2.34), one can express the parameters of PSGB in (2.16), (2.17) by the parameters of GB,

$$(2.35) \quad U(t) = |A(t)|^2 / \sqrt{(\pi\epsilon)^n |K|},$$

$$(2.36) \quad N_{11} = K + L^T K^{-1} L,$$

$$(2.37) \quad N_{12} = -L^T K^{-1},$$

$$(2.38) \quad N_{21} = -K^{-1} L$$

$$(2.39) \quad N_{22} = K^{-1}.$$

Next, we consider the Wigner transform for the summation of GBs. We only need to consider the case of a summation of two GBs:

$$\psi(t, \mathbf{x}) = \sum_{j=1}^2 \phi_j(t, \mathbf{x}) = \sum_{j=1}^2 A_j(\mathbf{x}) \exp \left[\frac{i}{\epsilon} \left(S_j + \mathbf{p}_j \cdot (\mathbf{x} - \mathbf{q}_j) + \frac{1}{2} (\mathbf{x} - \mathbf{q}_j)^T M_j (\mathbf{x} - \mathbf{q}_j) \right) \right],$$

whose Wigner transform is

$$\begin{aligned} W^\epsilon(t, \mathbf{x}, \mathbf{k}) &= \frac{1}{(2\pi)^n} \int_{\mathbb{R}^n} e^{i\mathbf{k} \cdot \tilde{\mathbf{x}}} \psi(t, \mathbf{x} - \frac{\epsilon}{2} \tilde{\mathbf{x}}) \overline{\psi(t, \mathbf{x} + \frac{\epsilon}{2} \tilde{\mathbf{x}})} d\tilde{\mathbf{x}} \\ &= \frac{1}{(2\pi)^n} \int_{\mathbb{R}^n} e^{i\mathbf{k} \cdot \tilde{\mathbf{x}}} (\phi_1^- + \phi_2^-) \overline{(\phi_1^+ + \phi_2^+)} d\tilde{\mathbf{x}} \\ &= \frac{1}{(2\pi)^n} \int_{\mathbb{R}^n} e^{i\mathbf{k} \cdot \tilde{\mathbf{x}}} (\phi_1^- \overline{\phi_1^+} + \phi_2^- \overline{\phi_1^+} + \phi_1^- \overline{\phi_2^+} + \phi_2^- \overline{\phi_2^+}) d\tilde{\mathbf{x}} \\ &= \mathfrak{W}[\phi_1^-, \overline{\phi_1^+}] + \mathfrak{W}[\phi_2^-, \overline{\phi_2^+}] + \mathfrak{W}[\phi_1^-, \overline{\phi_2^+}] + \mathfrak{W}[\phi_2^-, \overline{\phi_1^+}], \end{aligned}$$

where

$$\phi_j^\pm = \phi_j(\mathbf{x} \pm \frac{\epsilon}{2} \tilde{\mathbf{x}}), \quad j = 1, 2.$$

The Wigner transform for ϕ_1, ϕ_2 is known from (2.34). The rest is to derive the formula for the crossing terms $\phi_2^- \overline{\phi_1^+}$ and $\phi_1^- \overline{\phi_2^+}$. We first calculate

$$\frac{1}{(2\pi)^n} \int_{\mathbb{R}^n} e^{i\mathbf{k} \cdot \tilde{\mathbf{x}}} \phi_2^- \overline{\phi_1^+} d\tilde{\mathbf{x}} = \frac{\overline{A_1} A_2}{(2\pi)^n} e^{-\frac{(\mathbf{x}-\mathbf{q}_1)^T K_1 (\mathbf{x}-\mathbf{q}_1) + (\mathbf{x}-\mathbf{q}_2)^T K_2 (\mathbf{x}-\mathbf{q}_2)}{2\epsilon}} \int_{\mathbb{R}^n} e^{i\mathbf{k} \cdot \tilde{\mathbf{x}}} e^{i\tau_{12}/\epsilon} e^{i\tau(\tilde{\mathbf{x}})} e^{g(\tilde{\mathbf{x}})} d\tilde{\mathbf{x}},$$

with

$$\begin{aligned} L_j &= \text{Re}(M_j), \quad K_j = \text{Im}(M_j), \quad j = 1, 2, \\ \tau_{12} &= (S_2 - S_1) + (\mathbf{p}_2 \cdot (\mathbf{x} - \mathbf{q}_2) - \mathbf{p}_1 \cdot (\mathbf{x} - \mathbf{q}_1)) \\ &\quad + \frac{1}{2} ((\mathbf{x} - \mathbf{q}_2)^T L_2 (\mathbf{x} - \mathbf{q}_2) - (\mathbf{x} - \mathbf{q}_1)^T L_1 (\mathbf{x} - \mathbf{q}_1)), \\ \tau(\tilde{\mathbf{x}}) &= \frac{1}{2} [(\mathbf{p}_1 + \mathbf{p}_2) + L_2 (\mathbf{x} - \mathbf{q}_2) + L_1 (\mathbf{x} - \mathbf{q}_1)] \cdot \tilde{\mathbf{x}} + \frac{\epsilon}{8} \tilde{\mathbf{x}}^T (L_2 - L_1) \tilde{\mathbf{x}}, \\ g(\tilde{\mathbf{x}}) &= -\frac{\epsilon}{8} \tilde{\mathbf{x}}^T (K_2 + K_1) \tilde{\mathbf{x}} + \frac{1}{2} (K_1 (\mathbf{x} - \mathbf{q}_1) - K_2 (\mathbf{x} - \mathbf{q}_2)) \cdot \tilde{\mathbf{x}}. \end{aligned}$$

After a tedious but trivial calculation, one gets

$$\begin{aligned} \mathfrak{W}[\phi_2^-, \overline{\phi_1^+}] &= \frac{\overline{A_1} A_2}{\sqrt{(\frac{\pi\epsilon}{2})^n |i(M_2 - M_1)|}} e^{[-\frac{1}{2\epsilon} ((\mathbf{x}-\mathbf{q}_1)^T K_1 (\mathbf{x}-\mathbf{q}_1) + (\mathbf{x}-\mathbf{q}_2)^T K_2 (\mathbf{x}-\mathbf{q}_2)) + i\frac{\tau_{12}}{\epsilon}]} \\ &\quad \times e^{[\frac{2i}{\epsilon} (\mathbf{k} - \hat{\mathbf{p}} + \frac{i}{2} (K_2 (\mathbf{x}-\mathbf{q}_2) - K_1 (\mathbf{x}-\mathbf{q}_1)))^T (M_2 - M_1)^{-1} (\mathbf{k} - \hat{\mathbf{p}} + \frac{i}{2} (K_2 (\mathbf{x}-\mathbf{q}_2) - K_1 (\mathbf{x}-\mathbf{q}_1)))]}, \end{aligned}$$

where

$$\hat{\mathbf{p}} = \frac{\mathbf{p}_1 + \mathbf{p}_2}{2} + \frac{1}{2}(K_2(\mathbf{x} - \mathbf{q}_2) + K_1(\mathbf{x} - \mathbf{q}_1)).$$

From the fact

$$\mathfrak{W}[\phi_1^-, \overline{\phi_2^+}] = \overline{\mathfrak{W}[\phi_2^-, \overline{\phi_1^+}]},$$

the summation of the crossing terms in the Wigner transform of two GBs is

$$(2.40) \quad \mathfrak{W}[\phi_1^-, \overline{\phi_2^+}] + \mathfrak{W}[\phi_2^-, \overline{\phi_1^+}] = 2\text{Re}(\mathfrak{W}[\phi_2^-, \overline{\phi_1^+}]),$$

which represent the interference between different GBs.

Until now, we are able to get the Wigner transform of the initial data. Using the relations (2.35)-(2.39), again, one can derive the evolution equations for the parameters of PSGBs from (2.11)-(2.15):

$$(2.41) \quad \dot{\mathbf{q}} = \mathbf{p},$$

$$(2.42) \quad \dot{\mathbf{p}} = -\nabla_{\mathbf{q}} V,$$

$$(2.43) \quad \dot{U} = 0,$$

$$(2.44) \quad \dot{N}_{11} = \nabla_{\mathbf{q}}^2 V N_{12} + N_{21} \nabla_{\mathbf{q}}^2 V,$$

$$(2.45) \quad \dot{N}_{12} = -N_{11} + \nabla_{\mathbf{q}}^2 V N_{22},$$

$$(2.46) \quad \dot{N}_{21} = -N_{11} + N_{22} \nabla_{\mathbf{q}}^2 V,$$

$$(2.47) \quad \dot{N}_{22} = -(N_{12} + N_{21}),$$

which are exactly the same as (2.26)-(2.28). Each PSGB proceeds with time and we can reconstruct $W^\epsilon(t, \mathbf{x}, \mathbf{k})$ at any fixed time by the summation of all PSGBs and their interferences. The details about the reconstruction will be described in section 4.

In summary, the initial value of the wave function in the physical space can be decomposed into the sum of GBs. After the Wigner transform, each GB is transformed into a PSGB, and the obtained parameters of these PSGBs will be used as the initial value of the ODE system (2.41)-(2.47). Namely, we solve the following initial value problem for each PSGB,

$$(2.48) \quad \dot{\mathbf{q}} = \mathbf{p}, \quad \mathbf{q}(0) = \mathbf{q}(0),$$

$$(2.49) \quad \dot{\mathbf{p}} = -\nabla_{\mathbf{q}} V, \quad \mathbf{p}(0) = \mathbf{p}(0),$$

$$(2.50) \quad \dot{U} = 0, \quad U(0) = |A(0)|^2 / \sqrt{(\pi\epsilon)^n |K(0)|},$$

$$(2.51) \quad \dot{N}_{11} = \nabla_{\mathbf{q}}^2 V N_{12} + N_{21} \nabla_{\mathbf{q}}^2 V, \quad N_{11}(0) = K(0) + (L^T K^{-1} L)(0),$$

$$(2.52) \quad \dot{N}_{12} = -N_{11} + \nabla_{\mathbf{q}}^2 V N_{22}, \quad N_{12}(0) = -(L^T K^{-1})(0),$$

$$(2.53) \quad \dot{N}_{21} = -N_{11} + N_{22} \nabla_{\mathbf{q}}^2 V, \quad N_{21}(0) = -(K^{-1} L)(0),$$

$$(2.54) \quad \dot{N}_{22} = -(N_{12} + N_{21}), \quad N_{22}(0) = K^{-1}(0).$$

Furthermore, the configuration of the PSGB will be preserved as time evolves, which can be seen as follows. From (2.36)-(2.39), we have

$$\begin{aligned} \mathbf{y}^T \tilde{M} \mathbf{y} &= \begin{bmatrix} \mathbf{x} \\ \mathbf{k} \end{bmatrix}^T \begin{bmatrix} K + L^T K^{-1} L & -L^T K^{-1} \\ -K^{-1} L & K^{-1} \end{bmatrix} \begin{bmatrix} \mathbf{x} \\ \mathbf{k} \end{bmatrix} \\ &= \mathbf{x}^T K \mathbf{x} + (L\mathbf{x} - \mathbf{k})^T K^{-1} (L\mathbf{x} - \mathbf{k}). \end{aligned}$$

From the theory of GB, K is positive definite if the initial data of K is positive definite. This indicates that the coefficient matrix \tilde{M} of the PSGB is positive definite if the coefficient matrix of the initial data is chosen to be positive definite.

Compared to the method in [14] which needs $O(\epsilon^{-n})$ Gaussian beams for the $2n$ dimensional Wigner equation, we only need $O(\epsilon^{-n/2})$ Gaussian beam due to the efficient initial data decomposition. Thus our method reduces the computational cost dramatically.

3. The interface conditions. If the potential $V(\mathbf{x})$ has some isolated discontinuities, the PSGB method will break down at these discontinuous points. Some interface conditions must be found to connect the PSGB at the interfaces. From the interface conditions for GB and the relations between GB and PSGB, one can find the interface conditions for PSGB.

We recall the interface conditions for GB [17, 43], Assume that the interface is a line (if $n = 2$) or a flat surface (if $n = 3$) locate at $q_1 = 0$. With \mathbf{q} , \mathbf{p} , A , M being the parameters as before, we introduce the following notations, see FIG. 3.1:

$$\text{Region 1 : } \{\mathbf{q} | q_1 < 0\}, \quad \mathbf{q}^- = [0^-, q_2, \dots, q_n], \quad V_1(\mathbf{q}^-) := \lim_{\mathbf{q} \rightarrow \mathbf{q}^-} V_1(\mathbf{q});$$

$$\text{Region 2 : } \{\mathbf{q} | q_1 > 0\}, \quad \mathbf{q}^+ = [0^+, q_2, \dots, q_n]. \quad V_2(\mathbf{q}^+) := \lim_{\mathbf{q} \rightarrow \mathbf{q}^+} V_2(\mathbf{q});$$

$$\text{the incident wave vector : } \mathbf{p}^i := (p_1^i, p_2, \dots, p_n);$$

$$\text{the reflected wave vector : } \mathbf{p}^r := (-p_1^i, p_2, \dots, p_n);$$

$$\text{the transmitted wave vector : } \mathbf{p}^t := (p_1^t, p_2, \dots, p_n),$$

$$\text{the amplitudes of the incident/transmitted/reflected beam : } A^i/A^t/A^r,$$

$$\text{the Hessian matrices of the incident/transmitted/reflected beam : } M^i/M^t/M^r.$$

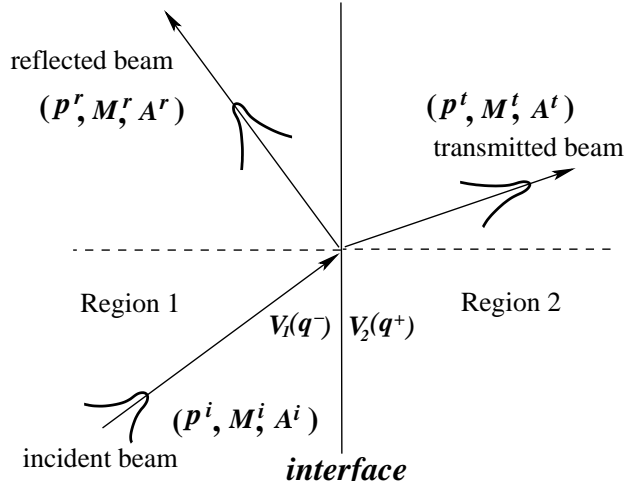


FIG. 3.1. beams at the interface

When the interface is as in Figure 3.1, the interface conditions for PSGB are given as follows. For wave vector \mathbf{p} , the Hamiltonian must be conserved,

$$(3.1) \quad p_2^r = p_2^i, \quad p_3^r = p_3^i, \quad \frac{1}{2}|\mathbf{p}^r|^2 + V_1(\mathbf{q}^-) = \frac{1}{2}|\mathbf{p}^i|^2 + V_1(\mathbf{q}^-),$$

$$(3.2) \quad p_2^t = p_2^i, \quad p_3^t = p_3^i, \quad \frac{1}{2}|\mathbf{p}^t|^2 + V_2(\mathbf{q}^+) = \frac{1}{2}|\mathbf{p}^i|^2 + V_1(\mathbf{q}^-).$$

The interface conditions for the amplitudes are

$$(3.3) \quad A^r = \alpha^r A^i, \quad \alpha^r = \frac{p_1^i - p_1^t}{p_1^i + p_1^t},$$

$$(3.4) \quad A^t = \alpha^t A^i, \quad \alpha^t = \frac{2p_1^i}{p_1^i + p_1^t}.$$

For Hessian matrices, one has

$$(3.5) \quad M^t = Q^t M^i Q^t - \frac{1}{p_1^t} \mathbf{e}_1 \mathbf{v}^T Q^t,$$

$$(3.6) \quad M^r = Q^r M^i Q^r,$$

where

$$Q^l = \begin{bmatrix} 1 & & \\ & 1 & \\ & & p_1^i/p_1^l \end{bmatrix}, \quad l = r, t, \quad \mathbf{v} = \nabla_{\mathbf{q}} V_2(\mathbf{q}^+) - \nabla_{\mathbf{q}} V_1(\mathbf{q}^-).$$

Then for $L = \text{Re}(M)$, $K = \text{Im}(M)$, we obtain the following interface conditions

$$(3.7) \quad K^l = Q^l K^i Q^l, \quad l = r, t.$$

$$(3.8) \quad L^t = Q^t L^i Q^t - \frac{1}{p_1^t} \mathbf{e}_3 \mathbf{v}^T Q^t,$$

$$(3.9) \quad L^r = Q^r L^i Q^r.$$

One can derive

$$|K^l| = |Q^l|^2 |K^i| = \left(\frac{p_1^i}{p_1^l}\right)^2 |K^i|, \quad l = r, t.$$

Combining the above equation with (2.35), we obtain the interface conditions for U ,

$$(3.10) \quad U^r = \beta^r U^i, \quad \text{with } \beta^r = \left| \frac{p_1^i - p_1^t}{p_1^i + p_1^t} \right|^2,$$

$$(3.11) \quad U^t = \beta^t U^i, \quad \text{with } \beta^t = \frac{p_1^i}{p_1^t} \cdot \frac{4p_1^i p_1^t}{|p_1^t + p_1^i|^2}.$$

For \mathbf{p} , the interface condition is the same as for GB's in (3.1) and (3.2).

On the other hand, from (2.36)-(2.39) and (3.7)-(3.9), we get the interface conditions for N ,

$$(3.12) \quad N_{11}^r = Q^r (N_{22}^i)^{-1} Q^r + Q^r (N_{21}^i)^T (N_{22}^i)^{-1} N_{21}^i Q^r, \\ N_{11}^t = Q^t (N_{22}^i)^{-1} Q^t + [Q^t (N_{21}^i)^T (N_{22}^i)^{-1} Q^t - \frac{1}{p_1^t} Q^t \mathbf{v}^T]$$

$$(3.13) \quad \cdot (Q^t)^{-1} N_{22}^i (Q^t)^{-1} [Q^t (N_{22}^i)^{-1} N_{21}^i - \frac{1}{p_1^t} \mathbf{e}_1 \mathbf{v}^T] Q^t,$$

$$(3.14) \quad N_{22}^l = (Q^l)^{-1} N_{22}^i (Q^l)^{-1}, \quad l = r, t,$$

$$(3.15) \quad N_{21}^t = (Q^t)^{-1} N_{21}^i Q^t + (Q^t)^{-1} N_{22}^i (Q^t)^{-1} \frac{1}{p_1^t} \mathbf{e}_1 \mathbf{v}^T Q^t,$$

$$(3.16) \quad N_{21}^r = (Q^r)^{-1} N_{21}^i Q^r.$$

We will use these interface conditions in our practical computations.

For the general case, one can apply the above techniques in the normal direction of the interface as in [29]. Take ξ_1, ξ_2 to be orthogonal coordinates on the interface. Defining $\Gamma(0, 0) = \Gamma_0$, we can define the interface near $\xi_1 = \xi_2 = 0$ as

$$(3.17) \quad \Gamma(\xi_1, \xi_2) = \Gamma_0 + \xi_1 \mathbf{t}_1 + \xi_2 \mathbf{t}_2 + \sum_{i,j=1}^2 C_{ij} \xi_i \xi_j \mathbf{t}_3,$$

where $\mathbf{t}_j, j = 1, 2$ are orthogonal unit vectors in the tangent plane at Γ_0 , and \mathbf{t}_3 is the unit normal of Γ at Γ_0 .

The interface conditions for the reflected GB are

$$(3.18) \quad \begin{aligned} \mathbf{p}^r \cdot \mathbf{t}_j &= \mathbf{p}^i \cdot \mathbf{t}_j, \quad j = 1, 2, \\ \frac{|\mathbf{p}^r|^2}{2} + V_1(\mathbf{q}^-) &= \frac{|\mathbf{p}^i|^2}{2} + V_1(\mathbf{q}^-), \end{aligned}$$

and the connection conditions for the transmitted wave

$$(3.19) \quad \begin{aligned} \mathbf{p}^t \cdot \mathbf{t}_j &= \mathbf{p}^i \cdot \mathbf{t}_j, \quad j = 1, 2, \\ \frac{|\mathbf{p}^t|^2}{2} + V_2(\mathbf{q}^+) &= \frac{|\mathbf{p}^i|^2}{2} + V_1(\mathbf{q}^-). \end{aligned}$$

For Hessian matrices M , the reflected GB satisfies

$$(3.20) \quad M^r = P_r^T M^i P_r,$$

where

$$P_r = Q_i Q_r^{-1}, \quad Q_j = (\mathbf{p}^j, \mathbf{t}_1, \mathbf{t}_2), \quad j = r, i,$$

and the transmitted GB satisfies

$$(3.21) \quad M^t = P_t^T M^i P_t + Q_t^{-T} D Q_t^{-1},$$

where

$$P_t = Q_t^{-T} Q_i, \quad Q_j = (\mathbf{p}^j, \mathbf{t}_1, \mathbf{t}_2), \quad j = i, t,$$

and

$$D = \begin{bmatrix} \mathbf{p}^i \cdot \nabla_{\mathbf{q}} V_1(\mathbf{q}^-) - \mathbf{p}^t \cdot \nabla_{\mathbf{q}} V_2(\mathbf{q}^+) & \mathbf{t}_1 \cdot \mathbf{v} & \mathbf{t}_2 \cdot \mathbf{v} \\ \mathbf{t}_1 \cdot \mathbf{v} & 2(\mathbf{p}^i - \mathbf{p}^t) \cdot \mathbf{t}_3 C_{11} & 2(\mathbf{p}^i - \mathbf{p}^t) \cdot \mathbf{t}_3 C_{12} \\ \mathbf{t}_2 \cdot \mathbf{v} & 2(\mathbf{p}^i - \mathbf{p}^t) \cdot \mathbf{t}_3 C_{21} & 2(\mathbf{p}^i - \mathbf{p}^t) \cdot \mathbf{t}_3 C_{22} \end{bmatrix}.$$

The amplitudes A are connected by the following conditions

$$(3.22) \quad A^r = \alpha^r A^i, \quad \alpha^r = \frac{(\mathbf{p}^i - \mathbf{p}^t) \cdot \mathbf{t}_3}{(\mathbf{p}^i + \mathbf{p}^t) \cdot \mathbf{t}_3},$$

$$(3.23) \quad A^t = \alpha^t A^i, \quad \alpha^t = \frac{2\mathbf{p}^i \cdot \mathbf{t}_3}{(\mathbf{p}^i + \mathbf{p}^t) \cdot \mathbf{t}_3}.$$

Then by using the relation between the GB and PSGB, one can derive the interface conditions for the PSGB.

$$(3.24) \quad U^r = \beta^r U^i, \quad \text{with } \beta^r = \left| \frac{(\mathbf{p}^i - \mathbf{p}^t) \cdot \mathbf{t}_3}{(\mathbf{p}^i + \mathbf{p}^t) \cdot \mathbf{t}_3} \right|^2 \cdot |P_r^{-1}|,$$

$$(3.25) \quad U^t = \beta^t U^i, \quad \text{with } \beta^t = \frac{4(\mathbf{p}^i \cdot \mathbf{t}_3)(\mathbf{p}^t \cdot \mathbf{t}_3)}{|(\mathbf{p}^i + \mathbf{p}^t) \cdot \mathbf{t}_3|^2} |P_t^{-1}|.$$

For \mathbf{p} , the interface conditions are the same as for GB's in (3.19) and (3.18).

The interface conditions for N are given as following

$$(3.26) \quad N_{11}^T = P_r^T (N_{22}^i)^{-1} P_r + P_r^T (N_{21}^i)^T (N_{22}^i)^{-1} N_{21}^i P_r,$$

$$(3.27) \quad N_{21}^T = P_r^{-1} N_{21}^i P_r,$$

$$(3.28) \quad N_{22}^T = P_r^{-1} N_{22}^i P_r^{-T},$$

$$(3.29) \quad N_{11}^t = P_t^T (N_{22}^i)^{-1} P_t + [Q_t^{-T} D Q_t^{-1} - P_t (N_{21}^i)^T (N_{22}^i)^{-1} P_t^T] \\ \cdot P_t^{-1} N_{22}^i P_t^{-T} [Q_t^{-T} D Q_t^{-1} - P_t (N_{22}^i)^{-1} N_{21}^i P_t],$$

$$(3.30) \quad N_{21}^t = P_t^{-1} N_{21}^i P_t - P_t^{-1} N_{22}^i P_t^{-T} Q_t^{-T} D Q_t^{-1},$$

$$(3.31) \quad N_{22}^t = P_t^{-1} N_{22}^i P_t^{-T}.$$

4. PSGB Summation. Now we reconstruct the approximate solution of the Wigner equation from PSGBs. One difficulty is that the phase information of GBs is lost in the Wigner transform. So one can not recover directly the interference terms of different PSGBs. We will recover the phase information from the parameters of the GB. The Wigner function of one single GB is a PSGB, which is always positive. However, the Wigner function of the sum of two GBs is not always positive. The negative part comes from the cross terms of these two beams.

In the reconstruction process, besides the summation of all the PSGBs, we need to add the crossing terms (2.40), namely, the solution is

$$(4.1) \quad W^\epsilon(t, \mathbf{x}, \mathbf{k}) = \sum_{j=1}^J U_j \exp\{-\frac{1}{\epsilon}(\mathbf{z} - \mathbf{z}_j)^T N_j (\mathbf{z} - \mathbf{z}_j)\} + \sum_{j,l=1, l < j}^J U_{jl}.$$

In order to find U_{jl} , we must express (2.40) by the parameters of PSGBs. From equations (2.36)-(2.39), one can write L_j and K_j as functions of $N_{lm}^{(j)}$, $l, m = 1, 2$,

$$L_j = -(N_{22}^{(j)})^{-1} N_{21}^{(j)}, \quad K_j = (N_{22}^{(j)})^{-1}, \quad j = 1, 2, \dots, J.$$

Thus, the crossing terms can be expressed by the parameters of PSGBs:

$$U_{jl} = \mathfrak{W}[\phi_j^- \overline{\phi_l^+}] = \frac{\overline{A_j} A_l}{\sqrt{(\frac{\pi\epsilon}{2})^n |i\tilde{M}_{jl}|}} e^{[-\frac{1}{2\epsilon}((\mathbf{x} - \mathbf{q}_l)^T (N_{22}^{(l)})^{-1} (\mathbf{x} - \mathbf{q}_l)) + (\mathbf{x} - \mathbf{q}_j)^T (N_{22}^{(j)})^{-1} (\mathbf{x} - \mathbf{q}_j)) + i\frac{\tau_{lj}}{\epsilon}]} \\ \times e^{[\frac{2i}{\epsilon}(\mathbf{k} - \hat{\mathbf{p}}_{jl} + \frac{i}{2}((N_{22}^{(j)})^{-1} (\mathbf{x} - \mathbf{q}_j) - (N_{22}^{(l)})^{-1} (\mathbf{x} - \mathbf{q}_l)))^T \tilde{M}_{lj}^{-1} (\mathbf{k} - \hat{\mathbf{p}}_{jl} + \frac{i}{2}((N_{22}^{(j)})^{-1} (\mathbf{x} - \mathbf{q}_j) - (N_{22}^{(l)})^{-1} (\mathbf{x} - \mathbf{q}_l)))]},$$

where

$$\tilde{M}_{lj} = -(N_{22}^{(j)})^{-1} N_{21}^{(j)} + i(N_{22}^{(j)})^{-1} + (N_{22}^{(l)})^{-1} N_{21}^{(l)} - i(N_{22}^{(l)})^{-1}, \\ \hat{\mathbf{p}}_{jl} = \frac{\mathbf{p}_l + \mathbf{p}_j}{2} + \frac{1}{2}((N_{22}^{(j)})^{-1} (\mathbf{x} - \mathbf{q}_j) + (N_{22}^{(l)})^{-1} (\mathbf{x} - \mathbf{q}_l)), \\ \tau_{lj} = (S_j - S_l) + (\mathbf{p}_j \cdot (\mathbf{x} - \mathbf{q}_j) - \mathbf{p}_l \cdot (\mathbf{x} - \mathbf{q}_l)) \\ - \frac{1}{2}((\mathbf{x} - \mathbf{q}_j)^T (N_{22}^{(j)})^{-1} N_{21}^{(j)} (\mathbf{x} - \mathbf{q}_j) + (\mathbf{x} - \mathbf{q}_l)^T (N_{22}^{(l)})^{-1} N_{21}^{(l)} (\mathbf{x} - \mathbf{q}_l)).$$

In the above formula, S_j and A_j , $j = 1, \dots, J$ include the phase information and can not be recovered directly. From the equations of GB, we know

$$(4.2) \quad \dot{S}_j(t) = \frac{1}{2} |\mathbf{p}_j|^2 - V(\mathbf{q}_j),$$

$$(4.3) \quad \dot{A}_j(t) = -\frac{1}{2} (\text{Tr}(M_j)) A_j(t).$$

Since

$$|A_j(t)|^2 = U_j(t) \sqrt{(\pi\epsilon)^n |K_j|} = U_j(t) \sqrt{(\pi\epsilon)^n |(N_{22}^{(j)})^{-1}|}, \quad 0 \leq j \leq J,$$

we can rewrite $A_j(t) = |A_j(t)|e^{\Phi_j}$, then

$$(4.4) \quad \dot{\Phi}_j(t) = -\frac{1}{2} \text{Tr}(K_j(t)) = -\frac{1}{2} \text{Tr}((N_{22}^{(j)})^{-1}(t)).$$

From (4.2) and (4.4), for $j = 1, \dots, N$, we obtain

$$(4.5) \quad S_j(t) = S_j(0) + \int_0^t \left[\frac{\mathbf{p}_j(\tau)^2}{2} - V(\mathbf{q}_j(\tau)) \right] d\tau,$$

$$(4.6) \quad \Phi_j(t) = \Phi_j(0) - \frac{1}{2} \int_0^t \text{Tr}((N_{22}^{(j)})^{-1}(\tau)) d\tau.$$

Finally, the crossing term can be recovered. The approximate solution $W(t, \mathbf{x}, \mathbf{k})$ obtained from the above summation can be negative due to the crossing term U_{jl} , which gives important corrections near the caustics.

We summarize our PSGB method as follows,

1. Decompose the initial wave function into a sum of GBs.
2. Define the centers $(\mathbf{q}_j(0), \mathbf{p}_j(0))$ of the GBs as the centers of PSGBs, and use the relations (2.35)-(2.39) to define the initial values of $U_j(t)$, $N_{11}^{(j)}(t)$, $N_{12}^{(j)}(t)$, $N_{21}^{(j)}(t)$, $N_{22}^{(j)}(t)$ for PSGB from the parameters of the corresponding GB.
3. Solve the ODE system (2.48) for each PSGB, and connect the beams at discontinuous points with interface conditions (3.12)-(3.16).
4. Use (4.1) to reconstruct the Wigner function $W^\epsilon(t, \mathbf{x}, \mathbf{k})$ from the PSGBs.

5. Numerical Examples. In this section we present four numerical examples to demonstrate the validity of our scheme and to show its numerical efficiency. In the numerical computations the fourth order Runge-Kutta time discretization is used.

EXAMPLE 5.1. Consider the 1-D Schrödinger equation (2.1) and (2.2). Let

$$V = 10, \quad A_0(x) = \exp(-25x^2), \quad S_0(x) = \frac{1}{5} \log(2 \cosh(5x)).$$

The corresponding Wigner equation is

$$(5.1) \quad \partial_t W^\epsilon(t, x, k) + k \cdot \nabla_x W^\epsilon(t, x, k) = 0,$$

with initial value defined by the Wigner transform of $\psi(0, \mathbf{x})$.

In this example, the reference solutions are computed by the time splitting spectral method for the Schrödinger equation in [7].

We choose $\epsilon = 1/1000$, the number of PSGBs is 150 and time step $\Delta t = 1/200$. FIG. 5.1 compares the position densities, the fluxes and the kinetic energies of the direct simulation of the Wigner equation and our PSGB method. The PSGB summation method provides an accurate approximation even in the region of the cusp caustics.

For different ϵ , FIG. 5.2 gives the l^1 and l^2 errors of the solution computed by the PSGB method for position density at time $t = 0.5$. We use 250 Gaussian beams and

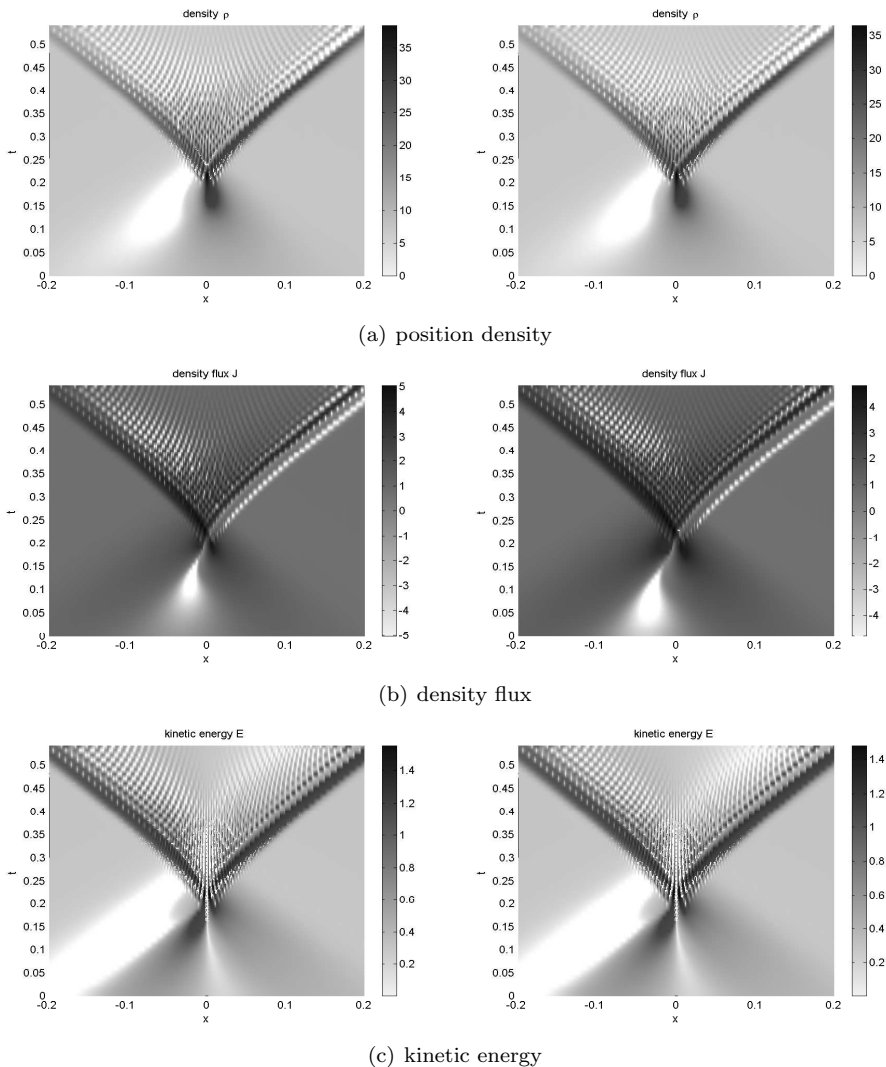


FIG. 5.1. Example 5.1. Evolution of solutions when $\epsilon = 1/1000$. Left: reference solution; right: approximate solution by PSGB method, using 150 PSGBs and $\Delta t = 1/200$.

$\Delta t = 1/1000$ in the PSGB method. The convergence rate of both l^1 and l^2 errors is about first order with respect to ϵ .

EXAMPLE 5.2. Consider the Schrödinger equation (2.1), (2.2), where

$$A_0(x) = \exp(-50(x + 0.2)^2), \quad S_0(x) = 1.6x, \quad V(x) = \begin{cases} 0, & x < 0.2, \\ 1, & x > 0.2, \end{cases}$$

the corresponding Wigner equation is

$$(5.2) \quad \partial_t W^\epsilon(t, x, k) + k \cdot \nabla_x W^\epsilon(t, x, k) + \mathfrak{L}^\epsilon W^\epsilon(t, x, k) = 0,$$

and initial condition is given by the Wigner transform of $\psi(0, \mathbf{x})$.

In this example, the potential contains a discontinuity at $x = 0.2$. We use 200 PSGBs to simulate the Wigner equation, and the time step is chosen to be $\Delta t = 1/200$.

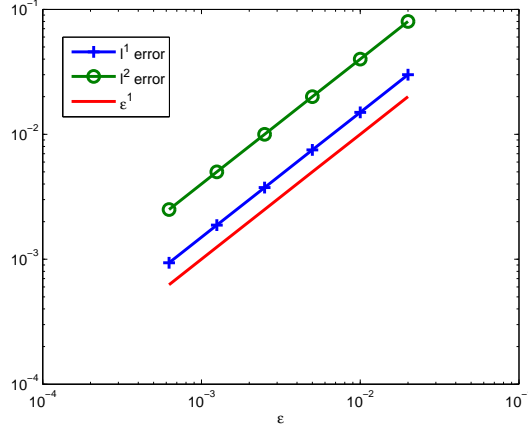


FIG. 5.2. Example 5.1: the convergence rate in ϵ of the l^1 and l^2 of the position density. Here we use 250 PSGBs and the time step is chosen as $1/1000$.

We need the interface conditions (3.12)-(3.16) to connect the reflected and transmitted PSGB to the incident PSGB.

For the sake of comparison, a reference solution for each potential is computed by the characteristic expansion method as in [43].

FIG. 5.3 shows the position density, fluxes and kinetic energies of the solution obtained by directly simulating the Wigner equation and the solution computed by our phase space Gaussian beam summation method. When an incident wave hits the singular point of the potential, it splits into a reflected wave and a transmitted wave. The PSGB method captures the reflected wave and transmitted wave accurately. The numerical results verify the validity of the interface conditions for PSGB.

FIG. 5.4 gives the l^1 and l^2 errors between the solution of the direct simulation of the Wigner equation and the solution computed by the PSGB method at time $t = 0.4$. We use 250 PSGBs and $\Delta t = 1/1000$. The convergence orders of both l^1 and l^2 errors are about one half with respect to ϵ . We have seen in Example 5.1 that the convergence order is 1 in ϵ when $V(x)$ is smooth, whereas in this example the order reduces to $1/2$ due to the discontinuities in $V(x)$.

EXAMPLE 5.3. Consider the Schrödinger equation (2.1), (2.2), when

$$A_0(x) = \exp(-100(x + 0.4)^2), S_0(x) = 1.8x, V(x) = \begin{cases} 0, & x < 0, \\ 1 - 0.2x, & 0 < x < 0.5, \\ -0.2x, & 0.5 < x < 1.5, \\ 1 - 0.2x, & 1.5 < x < 2, \\ -0.5, & x > 2, \end{cases}$$

the corresponding Wigner equation is

$$(5.3) \quad \partial_t W^\epsilon(t, x, k) + k \cdot \nabla_x W^\epsilon(t, x, k) + \mathfrak{L}^\epsilon W^\epsilon(t, x, k) = 0,$$

and the initial value is defined by the Wigner transform of $\psi(0, \mathbf{x})$.

The potential $V(x)$, as depicted in FIG. 5.5, possesses the form of the potentials for the resonant-tunneling diode (RTD) [10]. This kind of potentials appears in nanostructure and has been considerably explored in the field of semiconductor technology.

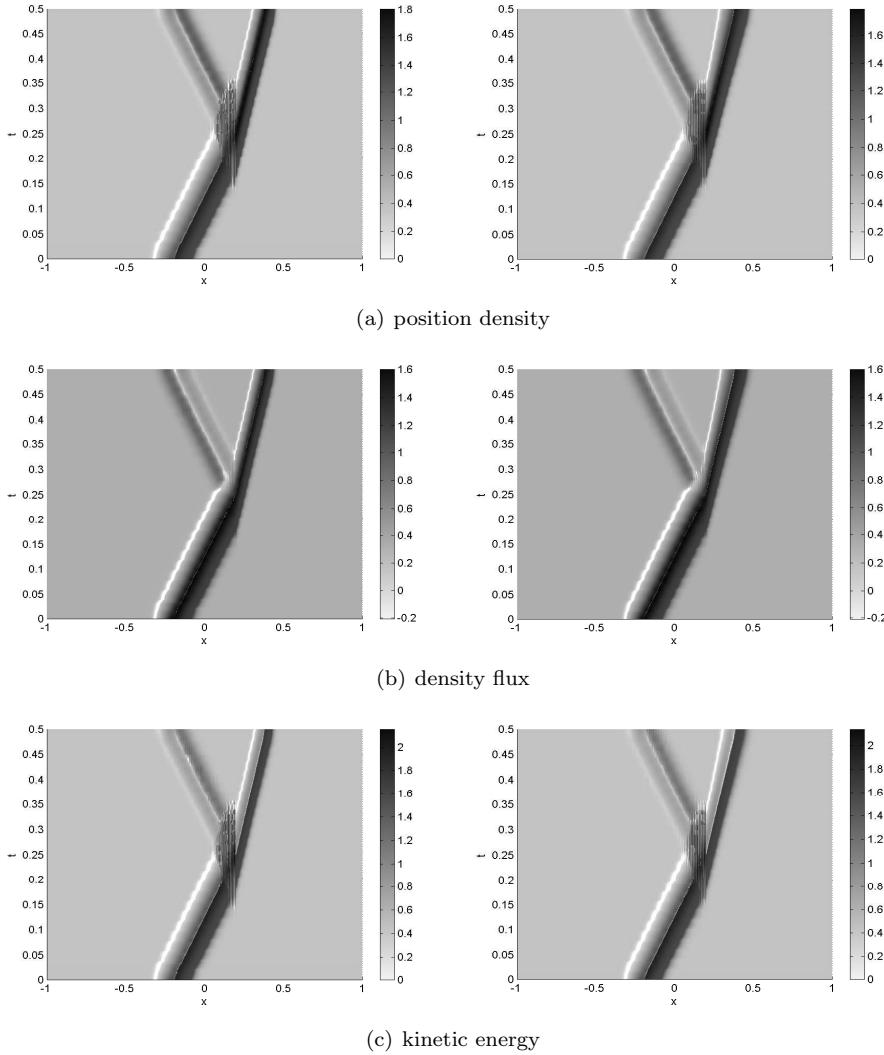


FIG. 5.3. Example 5.2. Evolution of solutions with $\epsilon = 1/1000$: left, the reference solution, right, the approximate solution by PSGB method

$V(x)$ has four discontinuities, and we need the interface conditions for PSGBs at these points. We use 200 phase space Gaussian beams to simulate the Wigner equation, and the time step is chosen to be $\Delta t = 1/200$. FIG. 5.6 shows the position density, fluxes and kinetic energies of the reference solution and the solutions computed by our PSGBs summation method. Thanks to the interface conditions, our method captures the reflected wave and transmitted wave accurately. The numerical results verify the validity of the interface conditions for PSGBs.

FIG.5.7 gives the l^1 and l^2 errors between the reference solution and the solution obtained by the phase space Gaussian beam method at time $t = 1.8$, where we use 200 PSGBs and the time step $\Delta t = 1/1000$. The convergence rates of both l^1 and l^2 errors are about half order in ϵ .

EXAMPLE 5.4. Finally, we consider the 2-D Schrödinger equation (2.1) and (2.2),

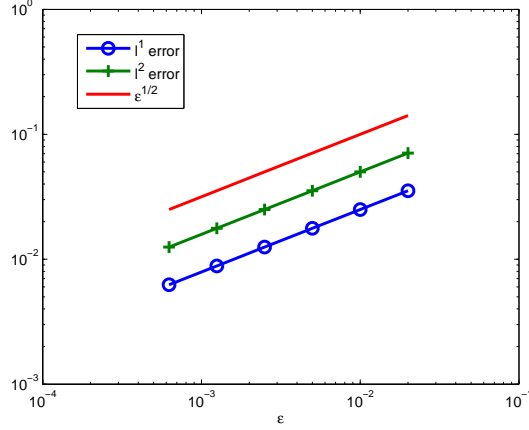


FIG. 5.4. Example 5.2: the convergence rate in ϵ of the l^1 and l^2 errors of the position density. Here we use 250 PSGBs and $\Delta t = 1/1000$.

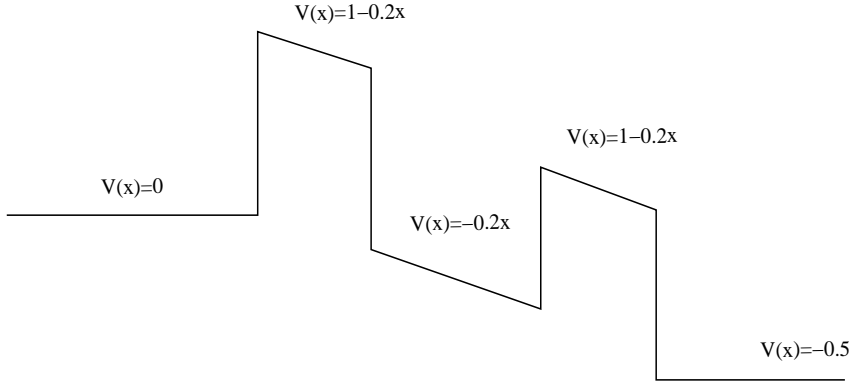


FIG. 5.5. Example 5.3: An electric potential $V(x)$ in Resonant Tunneling Diode.

where

$$A_0(x, y) = \exp(-100((x + 0.5)^2 + y^2)), \quad S_0(x, y) = 1.5x, \quad V(x, y) = \begin{cases} 0, & x < 0, \\ 1, & x > 0, \end{cases}$$

the corresponding Wigner equation is

$$(5.4) \quad \partial_t W^\epsilon(t, \mathbf{x}, \mathbf{k}) + \mathbf{k} \cdot \nabla_{\mathbf{x}} W^\epsilon(t, \mathbf{x}, \mathbf{k}) + \mathcal{L}^\epsilon W^\epsilon(t, \mathbf{x}, \mathbf{k}) = 0,$$

and initial condition is given by the Wigner transform of $\psi(0, \mathbf{x})$.

$V(x)$ has a jump at $x = 0$, so we need the interface conditions for PSGBs at this interface. In this example, a plane wave propagates from left to right, hits the interface and gives rise to a reflected wave and a transmitted wave. We use 200 phase space Gaussian beams to simulate the 2-D Wigner equation with $\epsilon = 1/400$, and the time step is chosen to be $\Delta t = 1/200$. FIG. 5.8 and FIG. 5.9 show the position density, fluxes and kinetic energies of the reference solution and the solution computed by our PSGBs summation method. Thanks to the interface conditions, our method captures

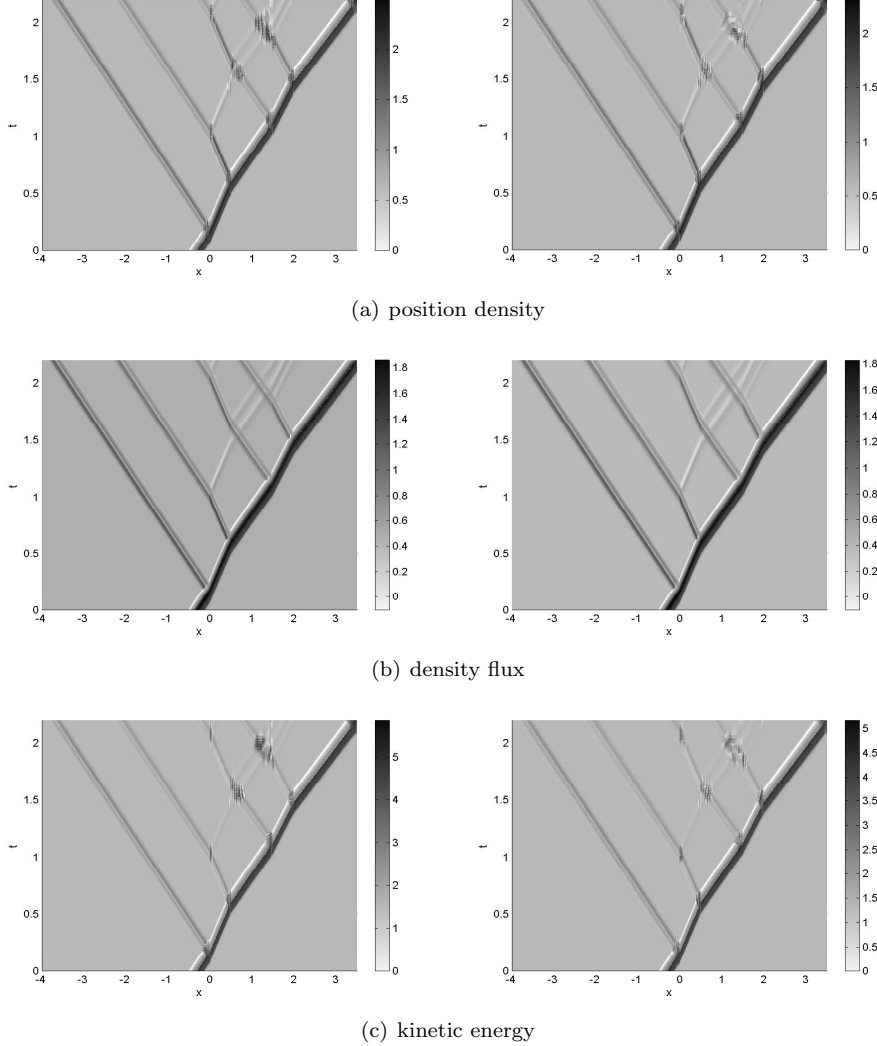


FIG. 5.6. Example 5.3. Evolution of solutions when $\epsilon = 1/1000$. Left: the reference solution; right: the approximate solution by our PSGB method, using 200 PSGBs and $\Delta t = 1/200$.

the reflected wave and transmitted wave accurately. The numerical results verify the validity of the interface conditions for PSGBs.

REMARK 1. *The direct simulations for $2n$ dimensional Wigner equation are very expensive. In order to resolve ϵ , the mesh size must be $O(\epsilon)$ and the time step have to be $O(\epsilon^{1/m})$, with m the convergence order of the time discretization. Thus, the total computational cost of direct simulation is of $O(\epsilon^{-2n-1/m})$.*

In the PSGB summation method for the $2n$ dimensional Wigner equation, the number of the PSGBs is $O(\epsilon^{-n/2})$, while the time step can be taken as $\Delta t = O(\epsilon^{1/2})$ in a fourth order time discretization. The computational cost of the summation process for the PSGBs is of $O(\epsilon^{-n/2})$. Therefore, the total computational cost of PSGB summation method is of $O(\epsilon^{-(n+1)/2})$.

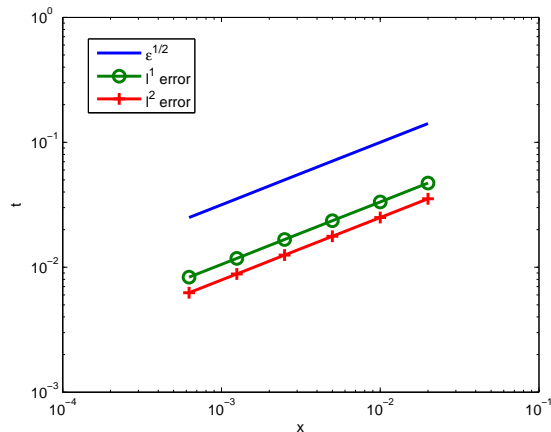


FIG. 5.7. Example 5.3: the convergence rate in ϵ of the l^1 and l^2 errors of the position density. Here we use 200 PSGBs and $\Delta t = 1/1000$.

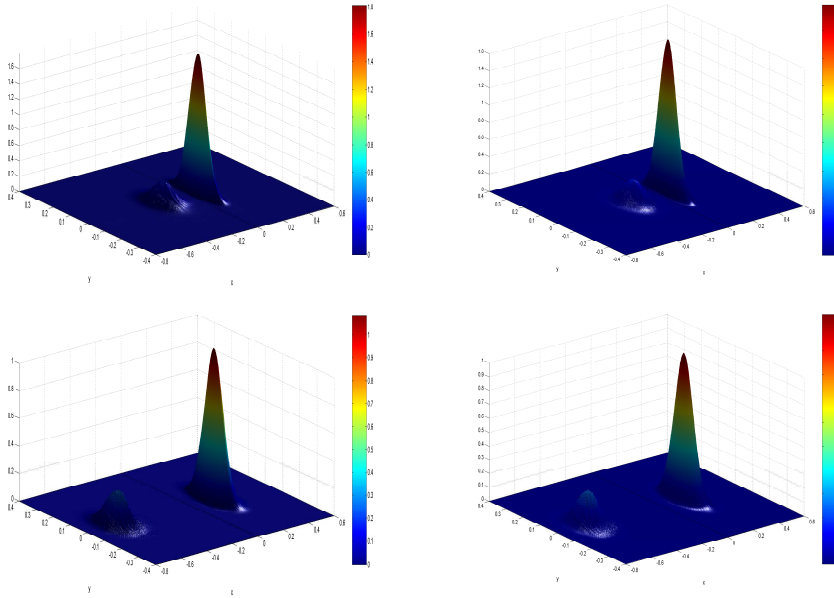
Therefore, the PSGB method significantly reduces the computational cost, and provide an accurate approximation to the Wigner equation, even with a discontinuous potential.

6. Conclusion. In this paper, We constructed a PSGB summation method for the Wigner equation with discontinuous potentials. By expanding the potential into a quadratic function locally, we derive the formulation of the PSGB method for the Wigner equation. We explore relations of the GB and the PSGB. Using these relations, we derive an efficient initial data decomposition method and the interface conditions for PSGBs and develop a summation method for the PSGBs. The computational cost of the PSGB method is much less than the direct simulation of the Wigner equation, but similar to the GB in physical space.

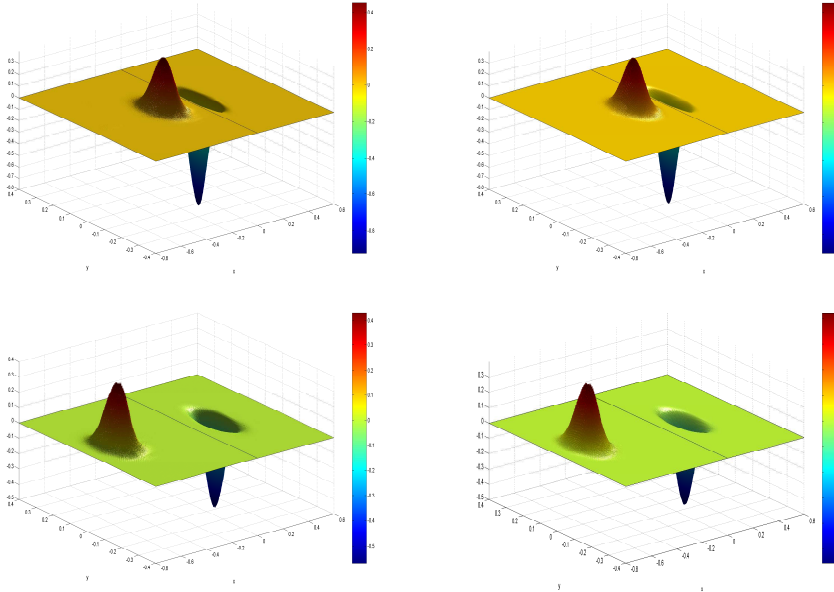
In the future, we will extend our method to the Wigner-Poisson and Wigner-Boltzmann equations.

REFERENCES

- [1] J. AKIAN, R. ALEXANDRE AND S. BOUGACHA, *A Gaussian beam approach for computing Wigner measures in convex domains*, *Kinet. Relat. Models.*, 4 (2011), no.3, pp. 589–631.
- [2] G. ARIEL, B. ENGQUIST, N. TANUSHEV AND R. TSAI, *Gaussian beam decomposition of high frequency wave fields using expectation-maximization*, *J. Comput. Phys.*, 230 (2011), p-p. 2303–2321.
- [3] A. ARNOLD AND F. NIER, *Numerical Analysis of the Deterministic Particle Method Applied to the Wigner Equation*, *Math. Comp.*, 58 (1992), no.198, pp. 645–669.
- [4] A. ARNOLD AND C. RINGHOFER, *Operator splitting methods applied to spectral discretizations of quantum transport equations*, *SIAM J. Numer. Anal.*, 32 (1995), pp. 1876–1894.
- [5] A. ARNOLD, H. LANGE, AND P. ZWEIFEL, *A discrete-velocity, stationary Wigner equation*, *J. Math. Phys.*, 41 (2000), pp. 7167–7180.
- [6] A. ARNOLD, *Mathematical properties of quantum evolution equations*, In *Quantum Transport-Modelling, Analysis and Asymptotics*, (eds. G. Allaire, A. Arnold, P. Degond, and T. Hou), *Lecture Notes Math.* Springer, Berlin, 1946 (2008), pp. 45–110.
- [7] W. BAO, S. JIN AND P. A. MARKOWICH, *On time-splitting spectral approximations for the Schrödinger equation in the semiclassical regime*, *J. Comput. Phys.*, 175 (2002), pp. 487–524.



(a) position density



(b) density flux

FIG. 5.8. *Example 5.4. Solutions when $\epsilon = 1/400$. Left: the reference solution; right: the approximate solution by our PSGB method, using 200 PSGBs and $\Delta t = 1/200$. Upper: $t = 0.4$, Lower: $t = 0.64$.*

[8] S. BOUGACHA, J. AKIAN, AND R. ALEXANDRE, *Gaussian beam summation for the wave equation in a convex domain*, Commun. Math. Sci., 7 (2009), pp. 973–1008.
 [9] L. DIECI AND T. EIROLA, *Positive definiteness in the numerical solution of Riccati differential*

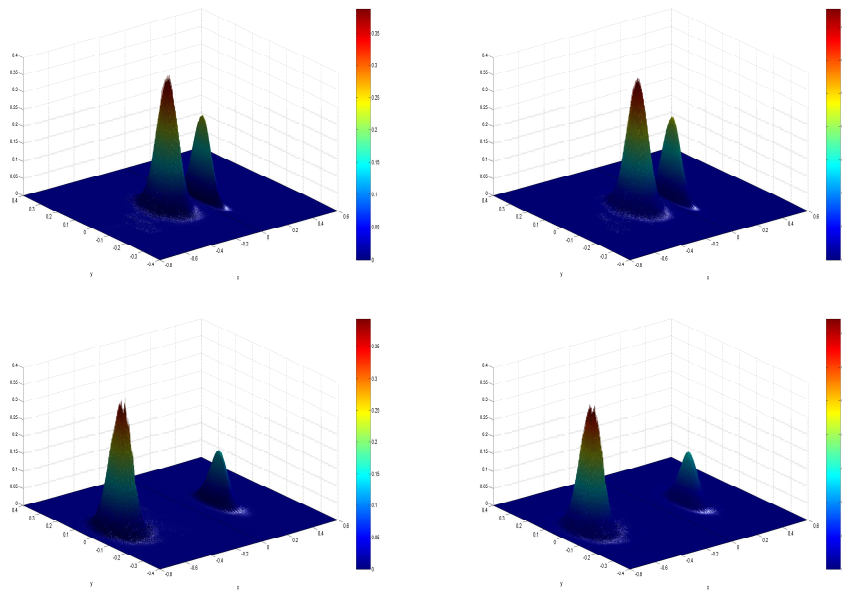


FIG. 5.9. Example 5.4. Kinetic energy when $\epsilon = 1/400$. Left: the reference solution; right: the approximate solution by our PSGB method, using 200 PSGBs and $\Delta t = 1/200$. Upper: $t = 0.4$, Lower: $t = 0.64$.

- equations, *Numer. Math.*, 67 (1994), no. 3, pp. 303–313.
- [10] W. FRENSLEY, *Wigner-function model of a resonant-tunneling semiconductor device*, *Phys. Rev. B*, 36 (1987), pp. 1570–1580.
- [11] P. GÉRARD, P. A. MARKOWICH, N. J. MAUSER, AND F. POUPAUD, *Homogenization limits and Wigner transforms*, *Comm. Pure Appl. Math.*, 50 (1997), pp. 321–379.
- [12] T. GOUDON, *Analysis of a semidiscrete version of the Wigner equation*, *SIAM J. Numer. Anal.*, 40 (2002), pp. 2007–2025.
- [13] E. J. HELLER, *Time-dependent approach to semiclassical dynamics*, *J. Chem. Phys.*, 62 (1975), no.4, pp. 1544–1555.
- [14] I. HORENKO, B. SCHMIDT AND C. SCHÜTTE, *Multidimensional classical Liouville dynamics with quantum initial conditions*, *J. Chem. Phys.*, 117 (2002), no.10, pp. 4643–4650.
- [15] N. KLUKSDAHL, A. KRIMAN, D. FERRY, AND C. RINGHOFER, *Self-consistent study of the resonant tunneling diode*, *Phys. Rev. B.*, 39 (1989), pp. 7720–7735.
- [16] S. JIN, P. MARKOWICH AND C. SPARBER, *Mathematical and computational methods for semiclassical Schrödinger equations*, *Acta Numerica*, 20 (2011), pp. 121–209.
- [17] S. JIN, D. WEI AND D. YIN, *Gaussian beam methods for the Schrödinger equation with discontinuous potentials*, preprint.
- [18] S. JIN, H. WU, AND X. YANG, *Gaussian beam methods for the Schrödinger equation in the semi-classical regime: Lagrangian and Eulerian formulations*, *Commun. Math. Sci.*, 6 (2008), pp. 995–1020.
- [19] H. KOSINA AND M. NEDJALKOV, *Wigner function-based device modeling*, In *Handbook of Theoretical and Computational Nanotechnology* (eds. M. Rieth and W. Schommers), American Scientific Publishers, Los Angeles, 10 (2006), pp. 731–763.
- [20] S. LEUNG AND J. QIAN, *Eulerian Gaussian beams for Schrödinger equations in the semi-classical regime*, *J. Comput. Phys.*, 228 (2009), pp. 2951–2977.
- [21] S. LEUNG, J. QIAN AND R. BURRIDGE, *Eulerian Gaussian beams for high-frequency wave propagation*, *Geophysics*, 72 (2007), no.5, pp. 61–76.
- [22] P.-L. LIONS AND T. PAUL, *Sur les mesures de Wigner*, *Rev. Mat. Iberoamericana*, 9 (1993), pp. 553–618.
- [23] H. LIU, O. RUNBORG AND N. M. TANUSHEV, *Error Estimates for Gaussian Beam Superpositions*, preprint.
- [24] P. MARKOWICH, C. RINGHOFER, AND C. SCHMEISER, *Semiconductor Equations*, Springer,

- Vienna, 1990.
- [25] P. MARKOWICH, *On the equivalence of the Schrödinger and the quantum Liouville equations*, Math. Meth. Appl. Sci., 11 (1989), pp. 459–469.
 - [26] M. MOTAMED AND O. RUNBORG, *Taylor expansion and discretization errors in Gaussian beam superposition*, Wave motion, 47 (2010), pp. 421–439.
 - [27] M. NEDJALKOV, R. KOSIK, H. KOSINA, AND S. SELBERHERR, *Wigner transport through tunneling structures-scattering interpretation of the potential operator*, In International Conference on Simulation of Semiconductor Processes and Devices SISPAD (2002), pp. 187–190.
 - [28] M. NEDJALKOV, D. VASILESKA, D. FERRY, C. JACOBONI, C. RINGHOFER, I. DIMOV, AND V. PALANOVSKI, *Wigner transport models of the electron-phonon kinetics in quantum wires*, Phys. Rev. B., 74 (2006), 035311.
 - [29] A. NORRIS, S. WHITE AND J. SCHRIEFFER, *Gaussian wave packets in inhomogeneous media with curved interfaces*, Pro. R. Soc. Lond. A, 412 (1987), pp. 93–123.
 - [30] M. M. POPOV, *A new method of computation of wave fields using Gaussian beams*, Wave Motion, 4 (1982), pp. 85–97.
 - [31] J. QIAN AND L. YING, *Fast Gaussian wavepacket transforms and Gaussian beams for the Schrödinger equation*, J. Comp. Phys., 229 (2010), pp. 7848–7873.
 - [32] J. RALSTON, *Gaussian beams and the propagation of singularities*, Studies in PDEs, MAA stud. Math., 23 (1982), pp. 206–248.
 - [33] U. RAVAIOLI, M. OSMAN, W. PÖTZ, N. KLUKSDAHL, AND D. FERRY, *Investigation of ballistic transport through resonant-tunnelling quantum wells using Wigner function approach*, Physica B., 134 (1985), pp. 36–40.
 - [34] C. RINGHOFER, *A spectral method for the numerical simulation of quantum tunneling phenomena*, SIAM J. Numer. Anal., 27 (1990), pp. 32–50.
 - [35] C. RINGHOFER, *Computational methods for semiclassical and quantum transport in semiconductor devices*, Acta Numerica., 6 (1997), pp. 485–521.
 - [36] D. ROBERT, *On the Herman-Kluk Semiclassical Approximation*, Rev. Math. Phys., 22 (2010), no.10, pp. 1123–1145.
 - [37] L. SHIFREN AND D. FERRY, *A Wigner function based ensemble Monte Carlo approach for accurate incorporation of quantum effects in device simulation*, J. Comp. Electr., 1 (2002), pp. 55–58.
 - [38] V. SVERDLOV, E. UNGERSBOECK, H. KOSINA, AND S. SELBERHERR, *Current transport models for nanoscale semiconductor devices*, Materials Sci. Engin. R., 58 (2008), pp. 228–270.
 - [39] N. M. TANUSHEV, B. ENGQUIST AND R. TSAI, *Gaussian beam decomposition of high frequency wave fields*, J. Comput. Phys., 228 (2009), pp. 8856–8871.
 - [40] N. M. TANUSHEV, J. L. QIAN AND J. RALSTON, *Mountain waves and Gaussian beams*, Multiscale Model. Simul, 6 (2007), pp. 688–709.
 - [41] N. M. TANUSHEV, *Superpositions and higher order Gaussian beams*, Commun. Math. Sci., 6 (2008), pp. 449–475.
 - [42] E. WIGNER, *On the quantum correction for the thermodynamic equilibrium*, Phys. Rev., 40 (1932), pp. 749–759.
 - [43] D. YIN AND C. ZHENG, *Gaussian beam formulation and interface conditions for the one-dimensional linear Schrödinger equation*, Wave Motion, 48 (2011), pp. 310–324.
 - [44] D. YIN AND C. ZHENG, *Composite coherent states approximation for one-dimensional multiphased wave functions*, Commun. Comput. Phys., 11 (2012), pp. 951–984.